The EMBO Journal (2012) 31, 2473–2485 | © 2012 European Molecular Biology Organization | All Rights Reserved 0261-4189/12
www.embojournal.org

THE EMBO JOURNAL

Drosophila midgut homeostasis involves neutral competition between symmetrically dividing intestinal stem cells

Joaquín de Navascués[1], Carolina N Perdigoto[2], Yu Bian[1], Markus H Schneider[3], Allison J Bardin[2], Alfonso Martínez-Arias[1] and Benjamin D Simons[4,5,*]

[1]Department of Genetics, University of Cambridge, Cambridge, UK, [2]Unité de Génétique et Biologie du Développement, Institut Curie, Paris, France, [3]Institut für Genetik, Heinrich-Heine-Universität, Düsseldorf, Germany, [4]Department of Physics, Cavendish Laboratory, University of Cambridge, Cambridge, UK and [5]The Wellcome Trust/Cancer Research UK Gurdon Institute, University of Cambridge, Cambridge, UK

The *Drosophila* adult posterior midgut has been identified as a powerful system in which to study mechanisms that control intestinal maintenance, in normal conditions as well as during injury or infection. Early work on this system has established a model of tissue turnover based on the asymmetric division of intestinal stem cells. From the quantitative analysis of clonal fate data, we show that tissue turnover involves the neutral competition of symmetrically dividing stem cells. This competition leads to stem-cell loss and replacement, resulting in neutral drift dynamics of the clonal population. As well as providing new insight into the mechanisms regulating tissue self-renewal, these findings establish intriguing parallels with the mammalian system, and confirm *Drosophila* as a useful model for studying adult intestinal maintenance.
The EMBO Journal (2012) **31,** 2473–2485. doi:10.1038/emboj.2012.106; Published online 20 April 2012
Subject Categories: development; differentiation & death
Keywords: intestinal homeostasis; lateral inhibition; neutral competition; population asymmetry; stochastic fate

Introduction

Understanding how the balance between proliferation and differentiation is controlled in adult tissues represents a defining question in stem cell biology (Watt and Hogan, 2000). Over the last few years, stem cells in the posterior midgut of adult *Drosophila* have been added to the inventory of systems in which to study such balance (Micchelli and Perrimon, 2006; Ohlstein and Spradling, 2006). This tissue contains two differentiated cell types: absorptive enterocytes (EC) and secretory enteroendocrine (EE) cells (Miller, 1950; Ohlstein and Spradling, 2006; Figure 1A and B). In homeostasis, these mature cells are constantly lost and replaced by new cells generated from intestinal stem cells (ISC) (Micchelli and Perrimon, 2006; Ohlstein and Spradling, 2006; Jiang and Edgar, 2009). Following early studies (Micchelli and Perrimon, 2006; Ohlstein and Spradling, 2006, 2007), it has been proposed that the *Drosophila* ISC divides to self-renew and give rise to an enteroblast (EB), which commits to differentiation without further division (Figure 1C). Notch (N) signalling emanating from the ISC, which specifically expresses the ligand Delta (Dl), is thought to instruct the committed fate to its EB sibling, which expresses an N activity reporter, *Su(H)GBE-lacZ*. Both ISCs and EBs are marked by the expression of the transcription factor escargot (esg) and arranged in small nests, enriched in Armadillo (Arm)/β-catenin and dispersed throughout the tissue (Micchelli and Perrimon, 2006; Ohlstein and Spradling, 2006; Figure 1B). Once they are defined, EBs differentiate into either an EC or EE cell depending on their signalling environment (Ohlstein and Spradling, 2006, 2007; Beebe *et al*, 2010; Liu *et al*, 2010; Figure 1C).

Following the early studies, the field has focussed primarily on the identification of the signalling pathways that control ISC behaviour during homeostasis and regeneration (reviewed in Apidianakis and Rahme, 2011 and Jiang and Edgar, 2011). However, the long-term lineage potential of ISCs is still not fully resolved. Most studies place emphasis on asymmetrical ISC division (leading to one ISC and one EB), although the molecular mechanism controlling asymmetrical fate allocation is unclear (reviewed in Hou, 2010; Karpowicz and Perrimon, 2010 and Fre *et al*, 2011). Indeed, direct evidence for intrinsically asymmetric ISC division or a symmetry-breaking mechanism shortly after division is so far lacking. Dl, a possible fate determinant molecule, does not segregate asymmetrically, and although the ISC division plane is tilted with respect to the basal membrane, there is no indication of a causal relationship with the fate of the daughter cells (Ohlstein and Spradling, 2007). Moreover, it has been reported that single cell-derived clones can contain more than one Dl^+ cell (Jiang *et al*, 2009), which is suggestive of symmetric fate outcome following division. A recent report using twin-spot labelling techniques has established that ISCs are capable of symmetric self-renewal, although the significance of this for homeostasis was left as an open question (O'Brien *et al*, 2011). Interestingly, in lineage tracing studies of homeostatic tissue (Ohlstein and Spradling, 2006) it is possible to observe seemingly unbound clonal expansion. Such behaviour contrasts with that expected from invariant asymmetry, where tissue should become organized into a mosaic of 'clonal units' (reminiscent of 'epidermal proliferative units' proposed as a model of mammalian interfollicular epidermis) (Potten, 1974, 1981). Since ISCs constitute some 18% of the total cell population (Micchelli and Perrimon, 2006), if all ISCs are active, then each one should support an average of

*Corresponding author. Department of Physics, Cavendish Laboratory, University of Cambridge, JJ Thomson Avenue, Cambridge CB3 0HE, UK. Tel.: +44 1223 334 095; Fax: +44 1223 337 356;
E-mail: bds10@cam.ac.uk

Received: 8 October 2011; accepted: 23 March 2012; published online 20 April 2012

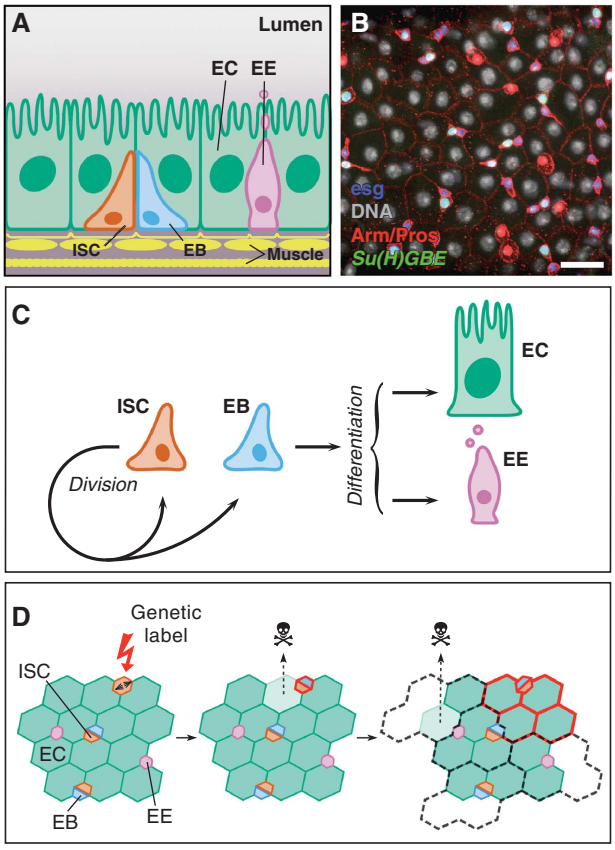

Figure 1 Composition and homeostasis of the adult posterior midgut. (**A**) Organization of the midgut epithelium in enterocytes (EC), enteroendocrine cells (EE), enteroblasts (EB) and intestinal stem cells (ISC), wrapped in muscle fibres. (**B**) View of the *Drosophila* midgut epithelium showing expression of Arm and Pros (red), *esg-lacZ* (blue), *Su(H)GBE-GFP:nls* (green) and DNA (grey pseudocolour). Separate channels are in Supplementary Figure S1. Bar: 20 μm. (**C**) Model of midgut homeostasis based on the asymmetric fate outcome of ISC division, and EB acting as a bipotent, non-amplifying precursor. (**D**) Predicted clonal evolution in invariant asymmetry. Long-lived clones arise by labelling (red) of an ISC. As tissue turns over, labelled clones grow until they occupy their 'proliferative unit'. Since ISCs lineages are immortal, labelled clones are bound by the proliferative unit; otherwise their expansion would be at the expense of the unlabelled lineages (discontinuous grey).

$(100-18)/18=4.6$ differentiated cells, leading to a clonal unit of 5–6 cells (Figure 1D). By contrast, Ohlstein and Spradling (2006) report wild-type clones reaching an average size of around 15 cells after 14 days post labelling, a behaviour consistent with typical wild-type clones presented in the literature (Lin *et al*, 2008, 2009; Lee *et al*, 2009; Beebe *et al*, 2010).

These observations led us to consider whether the balance between differentiation and division in *Drosophila* midgut was indeed achieved at the single-lineage level, or rather at the population level. In the latter termed *population asymmetry* (Watt and Hogan, 2000; Klein and Simons, 2011), ongoing ISC loss and replacement is engrained in the homeostatic process. To address this question, we undertook a detailed investigation of clonal fate in the adult *Drosophila* midgut. The analysis of a long-term clonal chase shows that tissue maintenance follows a pattern of population asymmetry whereby, following division, ISCs can give rise to either two ISCs, two EBs or one ISC and one EB, in a balanced manner. To further resolve details of the ISC population dynamics, we combine the long-term lineage tracing study with a detailed short-term analysis of the clonal composition. From these studies, we conclude that the balance between ISC proliferation and differentiation is maintained through a non cell-autonomous process, by which ISC loss is compensated by the symmetric duplication of neighbours. As well as determining the resulting frequency of ISC loss and replacement, we present evidence suggesting that the process of neutral competition is regulated at the molecular level by Dl/N-mediated lateral inhibition.

Results

Lineage composition is indicative of ISC loss and symmetric multiplication

To trace the lineages of individual cells, we made use of a heat shock-inducible genetic labelling system based on LacZ expression upon inter-chromosomal recombination (Harrison and Perrimon, 1993) (henceforth termed as *tub-FRT-lacZ* clones). This method has already been used in the adult gut (Ohlstein and Spradling, 2006) and was convenient for several reasons (see Supplementary Methods for details). Clones derived from unspecific (non-heat-induced) labelling were at least one order of magnitude less frequent than those induced through heat shock (Supplementary Figure S2A). The response of the labelling method to induction was remarkably uniform across the tissue (Supplementary Figure S2C and D). It was possible to identify individual clones with high confidence: we estimated that clone merger could have led to a misidentification of clones in $<2\%$ of cases (Supplementary Methods). Finally, as *tub-FRT-lacZ* clones are primarily induced upon mitosis (Harrison and Perrimon, 1993; Fox and Spradling, 2009), clones are expected to be founded mostly by the ISC progeny with a small number derived from post-mitotic cells (Supplementary Figure S2E). To avoid, as much as possible, non-homeostatic periods in the tissue due to post-emergence maturation or ageing (Biteau *et al*, 2008; O'Brien *et al*, 2011), the time window (in days of age, DOA, of the experimental flies) of all our lineage chasing experiments was between 3 and 23 DOA.

Using this approach we studied, at single-cell resolution, the evolution of clone size and density ($N=941$) over a 16-day time course (initiated at 5–7 DOA), as well as the internal clonal composition as measured by Dl expression and nuclear size in a smaller ($N=311$), separate, 5-day long chase (initiated at 3–6 DOA). As tissue turned over, we observed a gradual reduction in clone number and a progressive expansion of surviving clones (Figure 2A and B). If ISCs follow a pattern of invariant asymmetry, in which all divisions resulted in asymmetric fate outcome, then we would expect persisting clones to be derived from ISCs and just contain a single Dl^+ cell. Clones lost through the course of turnover would be derived from EBs and post-mitotic cells, and should remain as single cells until lost. When testing for this, we frequently found both single-cell clones and clones with one Dl^+ cell. However, we found that many clones bear two or more Dl^+ cells, while some multicellular clones contained no Dl^+ cells (Figures 3A–C, 4A and B). From

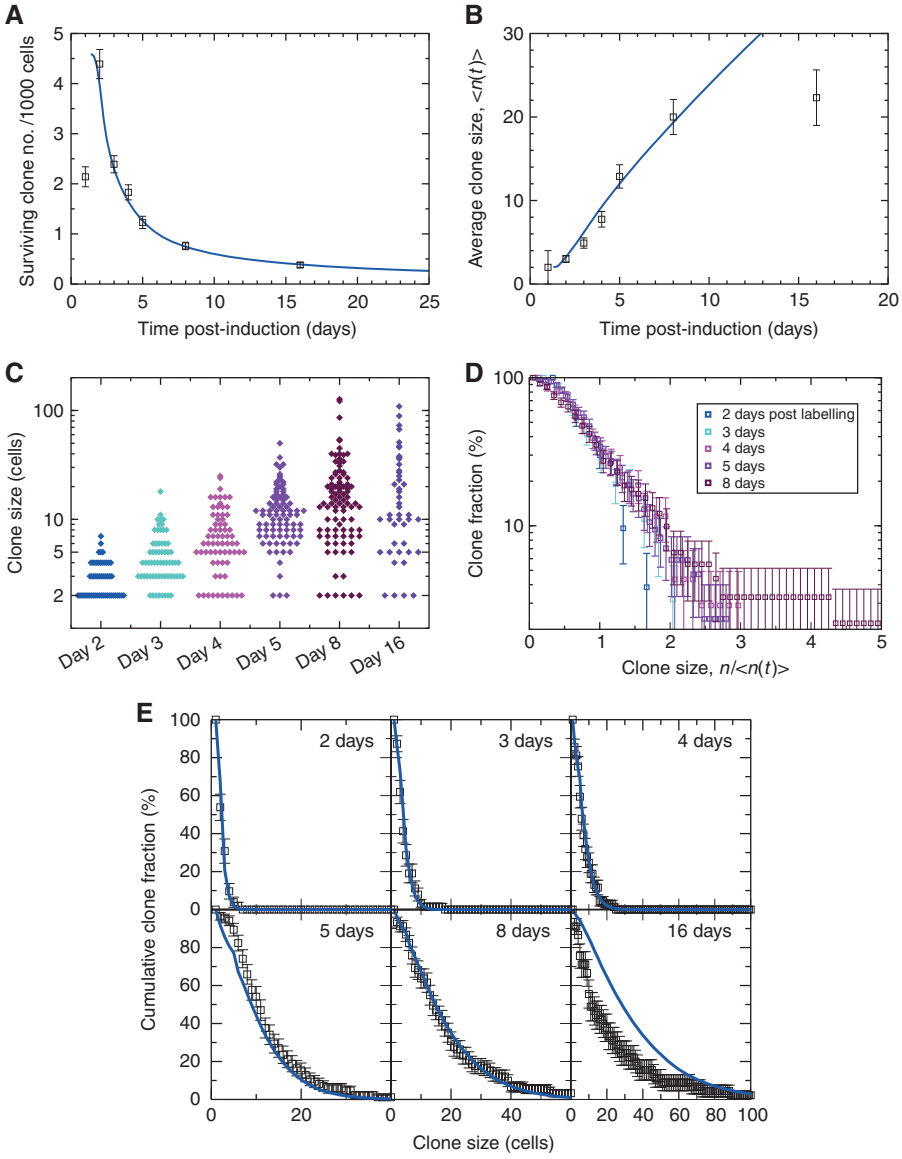

Figure 2 Long-term clone tracing shows loss and replacement with scaling behaviour. Blue curves show the predictions of the theoretical model for $\lambda = 2.5$/day and $r = 0.1$ (see main text). Error bars denote standard errors. To focus on ISC-derived clones, clone size distributions (**B**–**E**) consider only clones of two cells or more (see main text). (**A**, **B**) Evolution of clone density (**A**) and average clonal size (**B**). At maximal density (day 2), there is roughly one clone per 40 ISCs. To fit the theoretical curves (blue), we suppose that the induction frequency is 4.6 clones/1000 cells, and that the clonal expansion begins at 1.2 days (Supplementary Methods). (**C**) Raw clone size data between 2 and 16 days after labelling. Each diamond corresponds to one clone. (**D**) Plotted as a function of $n/<n(t)>$, the cumulative clone size distributions $C_n(t)$ (shown in **E**) derived from (**C**) converge at longer times onto a single scaling curve. This result shows that, despite the rapid increase in the average clone size, the chance of finding a clone larger than some multiple of the average remains constant over time. By presenting the data on a logarithmic scale, it is apparent that the cumulative size distribution follows an approximate exponential dependence on $n/<n(t)>$. (**E**) A comparison of the cumulative clone size distribution, $C_n(t)$, to the model defined in the main text shows an excellent agreement of theory (blue curve) with the data (points) both at short times and in the scaling regime. At 16 days post induction, the data depart from the predicted scaling behaviour of the model (see main text).

these observations, we conclude that ISC division can result in symmetric duplication and loss, as well in an asymmetric ISC/EB pair.

These observations were reinforced by the analysis of a twin-spot labelling method based on mitotic segregation, where sister clones are positively labelled by the expression of RFP and GFP, respectively (the 'twin-spot MARCM', Yu *et al*, 2009) (Figure 3D–G). With this labelling strategy, asymmetric ISC division should lead to the production of a single-cell clone of one colour in close proximity to its twin, which can expand to form a multi-cellular clone of the other colour. Indeed, although such clones were abundant (Figure 3E), we also found twin clones with multiple RFP^+ and GFP^+ cells (Figure 3F), in agreement with recent findings (O'Brien *et al*, 2011). Moreover, we also observed twin clones where both lineages were composed of single EC cells (Figure 3G). These results provide further and direct evidence of symmetric ISC duplication and loss, and were similarly reproduced (Supplementary Figure S3B and C) with two other twin-spot labelling methods (see Griffin *et al*, 2009 and Supplementary Figure S3D), all clones being induced at 4–7 DOA and chased for up to 3 days.

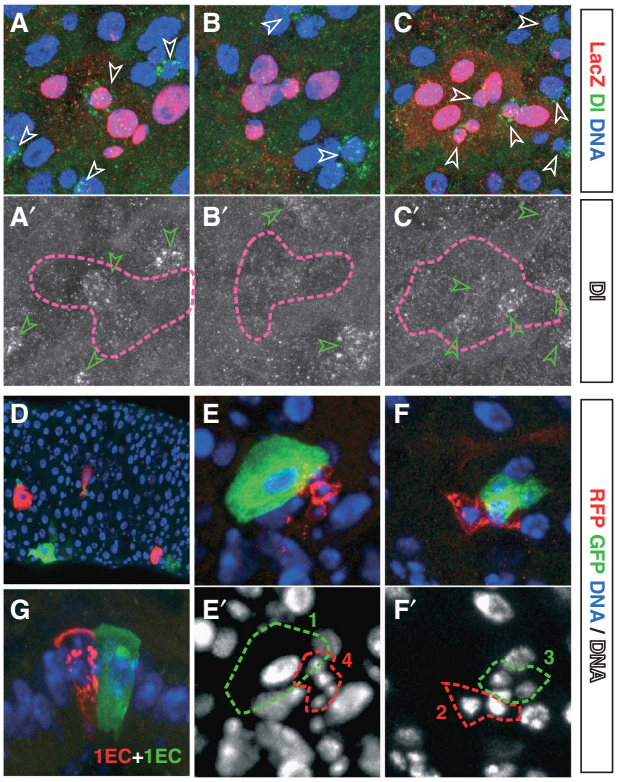

Figure 3 Lineage tracing shows divergence of fates. (**A**–**C**′) *tub-FRT-lacZ* clones (red/pink outline) labelled for Dl (green/white). Lineages based on Dl^+ cell (arrowheads) composition suggest divergent ISC fates; asymmetric (a single Dl^+ cell, **A**–**A**′), extinction (no Dl^+ cell, **B**–**B**′) or duplication (several Dl^+ cells, **C**–**C**′). (**D**–**G**) Twin-spot MARCM clones. (**D**) Tissue section with several small twin clones. The twin spots show asymmetric fate (**E**, one terminated clone containing a single EC and one multicellular clone), symmetric duplication (**F**, two multicellular clones) and symmetric differentiation (**G**, two single EC clones). (**E**′) and (**F**′) show DNA in greyscale and clone outlines in the corresponding colour. Clone in (**F**) is shown in wider field of view in Supplementary Figure S3A. Clones in (**A**–**C**, **F**) are provided as animated z-stacks in Supplementary Movies S1–S4.

These data provided strong evidence for all three possible fate outcomes following ISC division—two dividing cells, two committed cells, and one of each. However, these observations leave open the question of whether ISC loss and symmetrical self-renewal are features of normal homeostatic turnover, or rare events associated with chance injury and regeneration. To address this issue, we examined the entire cohort of surviving clones over the long-term time course in search of discriminating features.

Scaling behaviour of the clonal size distribution confirms neutral drift dynamics

Following heat shock, labelled clones showed a progressive expansion in average size alongside a reduction in density (Figure 2A and B). Superficially, such behaviour is consistent with invariant asymmetry: Clones founded by EBs would be transient, while ISC-derived clones would expand to occupy their 'clonal unit' (Figure 1D). However, if ISC division always led to asymmetric fate, then the clone density would stabilize at half the peak density, and the clone size saturate at the 5–6 cell average predicted by the tissue composition. By contrast, the data show a seemingly inexorable reduction

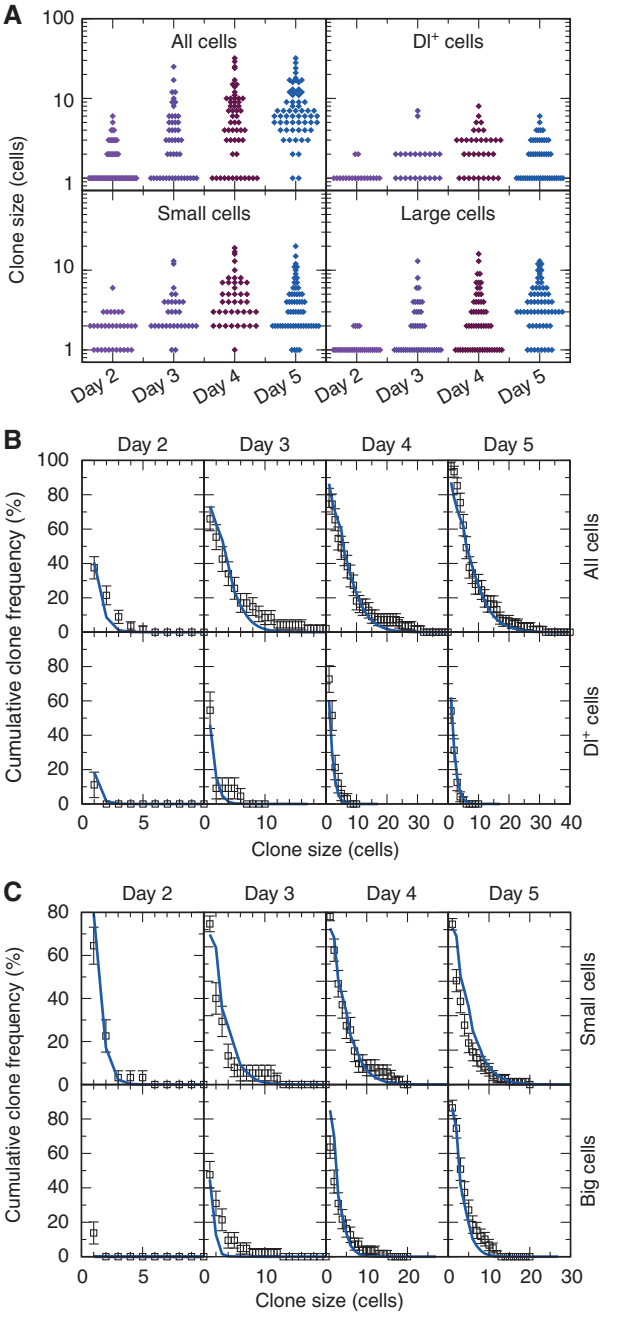

Figure 4 The model accurately predicts short-term lineage dynamics. (**A**) Raw clone size and cell-type composition data from the short-term lineage tracing (days 2–5 after labelling). Each diamond corresponds to one clone. (**B, C**) Cumulative distributions of clone total size and composition in Dl^+ cells (**B**), or small cells and large cells (**C**). The proposed model of neutral competition, with parameters $\lambda = 2.5$ and $r = 0.1$ (solid blue line), closely follows the data even in the early non-scaling regime (see main text).

in clone density (with some 91% of clones lost between day 2 and 16 post induction) combined with an increase in the average size of surviving clones (Figure 2A and B), consistent with observations reported in the literature (Ohlstein and Spradling, 2006). Furthermore, the full range of clone sizes (Figure 2C) included clones as large as 127 cells at 8 days post labelling, some 8 times larger than the average, or as small as two cells. From these observations, it is apparent that ISCs follow divergent fates. This could reflect an underlying

heterogeneity in the activity of ISCs, engrained during development or due to ageing, localized injury or infection. Alternatively, it could be indicative of 'neutral competition', whereby a functionally equivalent ISC population follows an unpredictable (stochastic) fate behaviour, which results in some clones expanding to replenish neighbours that are lost (Klein and Simons, 2011). To discriminate between these possibilities, we exploited a quantitative methodology previously developed to address clonal evolution in other homeostatic tissues (Clayton *et al*, 2007; López-García *et al*, 2010).

In tissues supported by an equipotent stem-cell population (a necessary condition of homeostatic tissue turnover) it has been shown that long-term clonal evolution must conform to one of only three possible classes of behaviour (Klein and Simons, 2011): invariant asymmetry, and two patterns of population asymmetry discriminated by whether the balance between stem-cell loss and duplication follows from intrinsic (cell autonomous) or extrinsic regulation. In both variants of population asymmetry, turnover leads to *neutral drift* in which clones expand to compensate neighbours that are lost. In turn, neutral competition leads to long-term 'scaling' of surviving clone size distributions, in which the chance of finding a clone larger than a multiple of the average remains constant over time.

More precisely, if we define $C_n(t)$ as the chance of finding a surviving clone with more than n cells at a time t post-labelling, then the size distribution is predicted to acquire the long-term scaling form (Klein and Simons, 2011), $C_n(t) = f(n/<n(t)>)$, where $<n(t)>$ represents the average size of the surviving clones and f denotes the scaling function. In an epithelial tissue, pertinent to the present system, the scaling function takes an exponential form, $f(x) = e^{-x}$. Scaling behaviour provides a robust signature of population asymmetry, as it reflects a property of the measured experimental data, and does not involve adjustment of any fitting parameters.

Significantly, when plotted against $n/<n(t)>$, the family of clone size distributions, $C_n(t)$ (Figure 2D and E), taken from different time points showed both collapse and convergence onto the same exponential form (Figure 2D, note the log scale). (Here, to eliminate transient clones founded through the induction of EB cells at the time of heat shock, we have focussed on the ensemble of clones comprising two cells or more, and therefore generated by an ISC; Supplementary Methods). From this observation it follows that, over the time course of the experiment, the tissue is maintained by population asymmetry. Importantly, from this behaviour, we can conclude that lineages with a composition indicative of symmetric duplication or ISC loss (Figures 3B, C, 4A and B), or twin spots with symmetric fates (Figure 3F and G), did not derive from rare processes involving localized injury or stress. Rather, these clones developed as part of normal homeostatic turnover in the midgut.

Although these results define a pattern of ISC turnover that represents an important departure from the model currently in use in the field, by itself, long-term scaling behaviour does not disclose details of the homeostatic process. In particular, it neither discriminates the pattern of regulation (intrinsic/extrinsic), nor the frequency of ISC loss and replacement. To address these questions, we must look for non-universal quantitative signatures in the detailed clonal fate data, prior to the onset of scaling. Therefore, we considered a physical model of the epithelium, built around the observation of scaling, tissue composition, and the known factors implicated in ISC regulation. From this model emerge quantitative predictions that can be challenged with experimental data.

A quantitative model of midgut epithelium turnover

To introduce the theoretical framework, it is useful to exploit the paradigm of invariant asymmetry both as a point of reference with which to compare separate modelling schemes, and as a platform to develop a model of population asymmetry. In a tissue maintained by invariant asymmetric self-renewal, an epithelium would become organized into a mosaic of clonal units that we term 'lineage domains' (Figure 1D). Applied to midgut, each domain would contain two undifferentiated cells (which constitute by number the esg^+ population), and an average of approximately four terminally differentiated cells (which constitute by number the ECs and EE cells). Since these domains do not constitute fixed anatomical boundaries, for simplicity, we will suppose that they are organized into a regular (square) two-dimensional (2D) array (Figure 5A). Of course, in the experimental system, the spatial distribution of ISCs appears to be random, while the geometry of the gut is cylindrical. However, our focus here is on the evolution of lineage composition over time, and not on the anatomical details of the tissue. Providing clones do not span the full circumference of the gut—which was always the case in our experiments—further refinements to accommodate the geometry and irregularity in the spatial organization of the tissue would only increase the complexity of the modelling scheme without providing significant new insight.

As tissue turns over, to maintain cell number through invariant asymmetry, the loss of a terminally differentiated cell must be compensated by the commitment of one of the esg^+ cells (the EB) to terminal differentiation alongside the cell division of its partner esg^+ cell (the ISC) in the same domain. In homeostasis, the division rate of the progenitor cells, λ, must therefore be perfectly matched by the differentiation and subsequent loss rate of terminally differentiated cells (Figure 5A). In a lineage tracing experiment, the induction of an ISC would result in the progressive expansion of the clone until its lineage domain had become fully labelled, while clones derived from differentiated cells would be lost through the course of turnover (Supplementary Figure S4A). As we have seen, such behaviour is inconsistent with both the lineage tracing data and the observed clonal composition.

Therefore, to accommodate the constraints presented by the clonal fate data, let us introduce a refinement of this 'classical' scheme that accommodates a degree of chance ISC loss and replacement. In particular, let us suppose that some ISC divisions result in the commitment to differentiation and cell-cycle exit of both progeny. If left unchecked, such a symmetrical fate outcome would, in turn, lead to the loss of all cells in the lineage domain. However, if such ISC loss is perfectly compensated by the symmetrical duplication of an ISC in a neighbouring domain, then cell number and local stem-cell density are conserved, and homeostasis is maintained (Figure 5B; Supplementary Figure S4B). Therefore, we will suppose that, with probability $1–2r$, terminal differentiation of an EB cell is compensated by ISC division within the

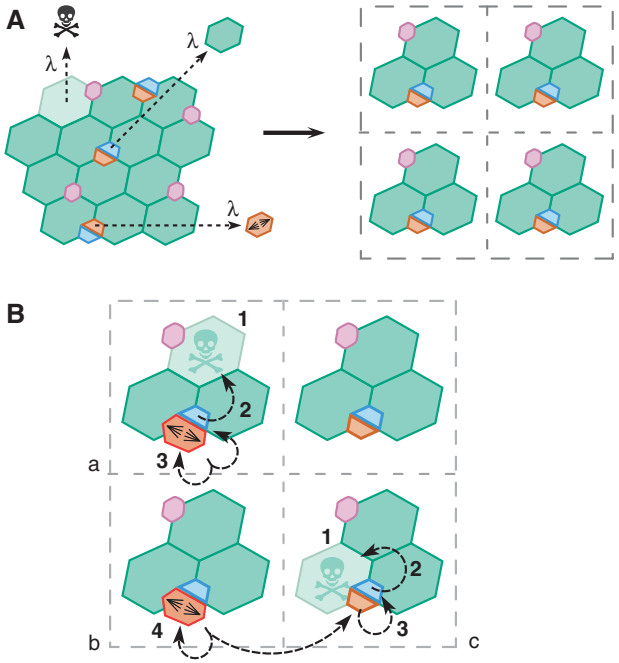

Figure 5 Quantitative model of tissue homeostasis. (**A**) The midgut epithelium is simplified as a square 2D lattice, each point containing two undifferentiated cells (by fraction, the ISC and EB population) and four mature, terminally differentiated cells (by fraction, three ECs and one EE cell). In homeostasis, the loss rate of mature terminally differentiated cells, λ, matches the differentiation rate of EB cells and the division rate of the ISCs. In a model of invariant asymmetric self-renewal, clones derived from differentiated cells will become progressively lost as the tissue turns over. Clones derived from ISCs will progressively expand to occupy the lineage domain/lattice point (see Figure 1D and Supplementary Figure S4A). (**B**) In the 2D lattice model, homeostasis takes place through a series of concatenated replacements. In domains (a) and (c), the loss of a mature terminally differentiated cell (1) triggers the differentiation of an EB (2). This EB loss, with probability $1-2r$, is replaced through division of the ISC (3) in the same domain (a). Alternatively, with probability $2r$, both undifferentiated cells within the domain (c) may commit to differentiation (3), which requires replacement to be fulfilled by the symmetrical duplication of an ISC (4) in a neighbouring domain (b).

same domain while, with probability $2r$, the sibling ISC is also lost through differentiation into an EB and is replaced through symmetrical division of an ISC in a neighbouring domain (Figure 5B; Supplementary Figure S4B). In this modelling scheme, the parameter r defines both the relative frequency of ISC division resulting in symmetrical loss and duplication.

Although the long-term dynamics implied by this model are known to converge onto the characteristic scaling behaviour reported above (Klein and Simons, 2011), the approach to scaling is inaccessible by analytical means. Fortunately, the cellular dynamics can be easily accessed by numerical simulation, allowing the short-term clonal evolution to be recovered straightforwardly by computer simulation. Taking a lattice of 500×500 lineage domains, more than sufficient to reach convergence, a comparison of the model with the data showed an excellent fit over the first 8 days following induction, if we set the ISC division rate to $\lambda = 2.5$/day and $r = 0.1$ (Figure 2E). With the same fitting parameters, a comparison of the average clone size and survival curve showed an equally good fit over the same time course (Figure 2A and B). When we adjusted λ and r keeping their product constant, we could still obtain a satisfactory fit to the data over a range of r between 0.07 and 0.13 with the value of 0.1 being optimal. From this result, we inferred that roughly 2 in 10 ISC divisions result in ISC loss and replacement. At 16 days post induction, we found departure of the data from some of the model predictions (Figure 2B and E), which we attribute to an ageing-related breakdown of homeostasis (see Discussion).

Clonal composition provides further support for the stochastic model

Alongside the total clone size, the model also made predictions about clonal composition. To further challenge the model, we considered a detailed analysis of the clonal composition over the first 5 days following heat shock (given at 3–6 DOA). In particular, we were able to identify and classify cells within labelled clones according to their expression of Dl, Pros, and whether the cell nuclei were small (diploid) or large (polyploid). At 5 days post induction, we find that $19 \pm 5\%$ of labelled cells are Dl^+ while some $7 \pm 4\%$ express Pros ($N = 61$) (see also Supplementary Table S2). These figures suggest that, by 5 days post induction, the population of labelled cells has become representative of the total cell population. At the same time, we find that the relative population of labelled cells with small and large nuclei are approximately equal with $50 \pm 6\%$ belonging to both groups. Taken together, these results are consistent with the majority of Dl^- $Pros^-$ small cells being EBs with only a few percent ECs. Therefore, we assumed that both the ISC and EB type cell, as well as one of the four terminally differentiated cells in the model belong to the population of small cells, with the remainder considered large.

From the raw experimental data (Supplementary Table S2), we compiled the size distribution of surviving clones disaggregated into the respective cell types (Figure 4A). The data showed a remarkably close agreement with that predicted by numerical simulation (Figure 4B and C, blue line), using the same values of λ and r obtained from fitting the long-term clonal fate data set.

As a final challenge to our quantitative model, we looked at Dl expression in clones chased for just 28 h (induced at 5–7 DOA). At this early time point, ISCs have undergone only a limited number of cell divisions, while terminally differentiated cells generated by the division of a marked ISC are expected to survive. The expression of Delta is potentially ambiguous shortly after division, given its even partition in the ISC offspring, followed by downregulation of Dl in the EB (Ohlstein and Spradling, 2007). However, the reduction of Dl levels in the EB is expected to occur rapidly in comparison with the ISC division rate. If Dl expression is resolved and limited to ISCs, in clones hosting only a small number of cells, then the relative contribution of symmetric and asymmetric cell divisions can be deduced unambiguously for the majority of these early clones (Figure 6A and C).

When looking at the distribution of the Dl^+ cells within the lineages, we observe the three possible fate outcomes Dl^+/Dl^+, Dl^-/Dl^- and Dl^+/Dl^- (Figure 6B i–vi). Importantly, the two symmetric outcomes, Dl^+/Dl^+ and Dl^-/Dl^-, appear balanced in number (indicating that Dl expression is indeed resolved), with 28 out of 161 divisions leading to symmetrical duplication, 104 leading to asymmetrical fate

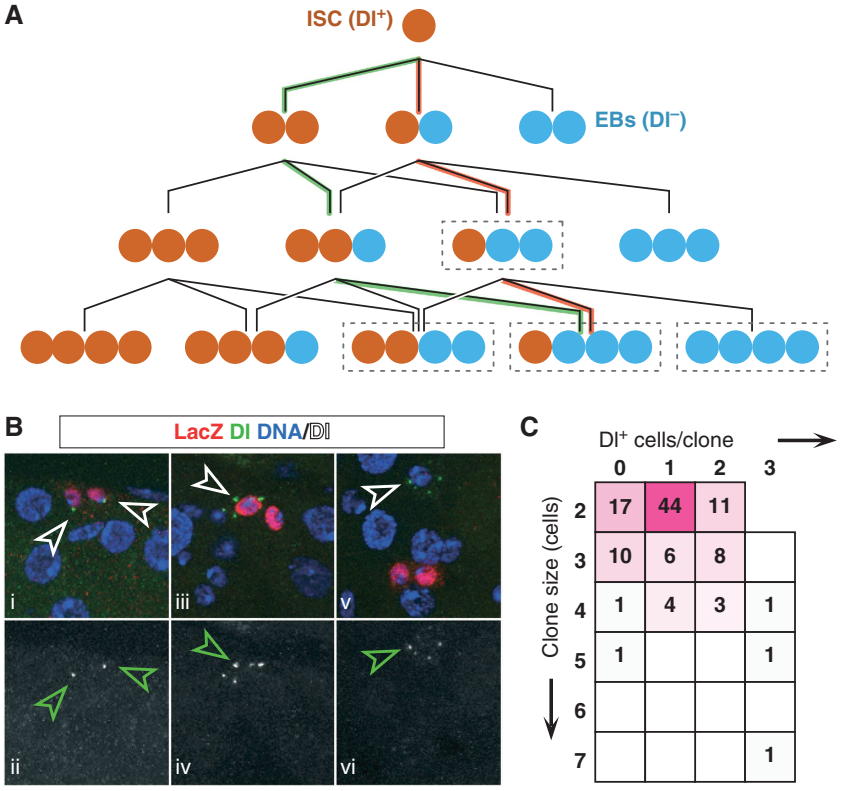

Figure 6 Twenty-eight hour lineage chase provides further evidence of neutral competition. (**A**) Lineage histories of different clone fates (in size and Dl^+ cell content). Cases in dashed boxes can be accessed through different histories: for instance, a 4-cell clone with one Dl^+ cell can originate from three consecutive asymmetric divisions (red pathway) or one asymmetric and two symmetric ones of opposing result (green pathway). All ambiguities are equivalent in terms of balance of symmetric duplication versus symmetric differentiation. (**B**) Two-cell clones showing the three different possible fates: symmetric duplication (two Dl^+ cells, i–ii), asymmetric (one Dl^+ cell, iii–iv) and symmetric differentiation (no Dl^+ cells, v–vi). (**C**) Matrix indicating the number of clones scored for each given clone size and given number of Dl^+ cells. Magenta hues represent relative frequencies of the scored events (magenta: 100%; white: 0%). Note that the majority of clones are of unambiguous lineage history (**A**).

and 29 leading to terminal division. Here, in the few cases where the fate assignation is ambiguous, we have maximized the asymmetric lineage combination, which is in the majority. As well as providing independent confirmation of tissue homeostasis and the neutrality of the competition between ISCs, the relative proportion of symmetric to asymmetric fate outcomes is set at around 1 in 3, a frequency somewhat higher than predicted by the long-term clonal fate data, but within the error of the measurement. Therefore, taken together, all lineage tracing experiments are consistent with ISC self-renewal involving frequent loss and replacement, with the balance between proliferation and differentiation following from external regulation.

Composition of nests of esg^+ cells is compatible with ISC loss and replacement

If ISCs are undergoing symmetric duplication and differentiation, then this should leave a mark in the spatial organization of ISCs and EBs in the epithelium, and in particular in their arrangement in nests. To test this, we examined 980 esg^+ cell nests (comprising 1502 cells) in flies 3–5 days old, and recorded their size and composition in Su(H)GBE^+ cells. We defined a nest as a group of esg^+ cells that share at least one vertex of Arm-enriched membrane (Ohlstein and Spradling, 2006), and considered esg^+ Su(H)GBE^+ cells to be EBs, and esg^+ Su(H)GBE^- cells as ISCs (Micchelli and Perrimon, 2006; Ohlstein and Spradling, 2007; Choi *et al*, 2011; O'Brien *et al*, 2011; Wang *et al*, 2011; Xu *et al*, 2011). As expected, nests were homogeneously distributed across the epithelium (Figure 1B), with every nest having its closest neighbour within 55 μm (Figure 7H). While the populations of ISCs and EBs were balanced at the global scale (ISC/EB ratio = 1.04; Supplementary Table S1), individual nests had variable size and composition (Figure 7A–G; Supplementary Table S1).

Nests were mostly comprising single or paired cells, with some trios and a few quartets (Figure 7G). We found four larger clusters, which we did not consider further. Of the 976 clusters composed of one to four cells, 660 (68%) were composed of a single ISC isolated or accompanied by one to three EBs (Figure 7A–C and F), which is compatible with a majority of ISC divisions being asymmetric. However, 271 nests (28%) of sizes ranging one to three cells were composed entirely of EBs (Figure 7A, D and F). From this observation, it follows that the esg^+ nests may lose all supporting ISCs, which is compatible with ISCs undergoing symmetric differentiation. We also found 45 nests (11% of the multicellular ones) containing more than one ISC (Figure 7B, E and F), which is in agreement with our observation of ISC symmetric duplication. Alternatively, it could be a signature of nest merger. Therefore, we considered whether ISCs in the tissue are typically closest to an EB, regardless of their nest

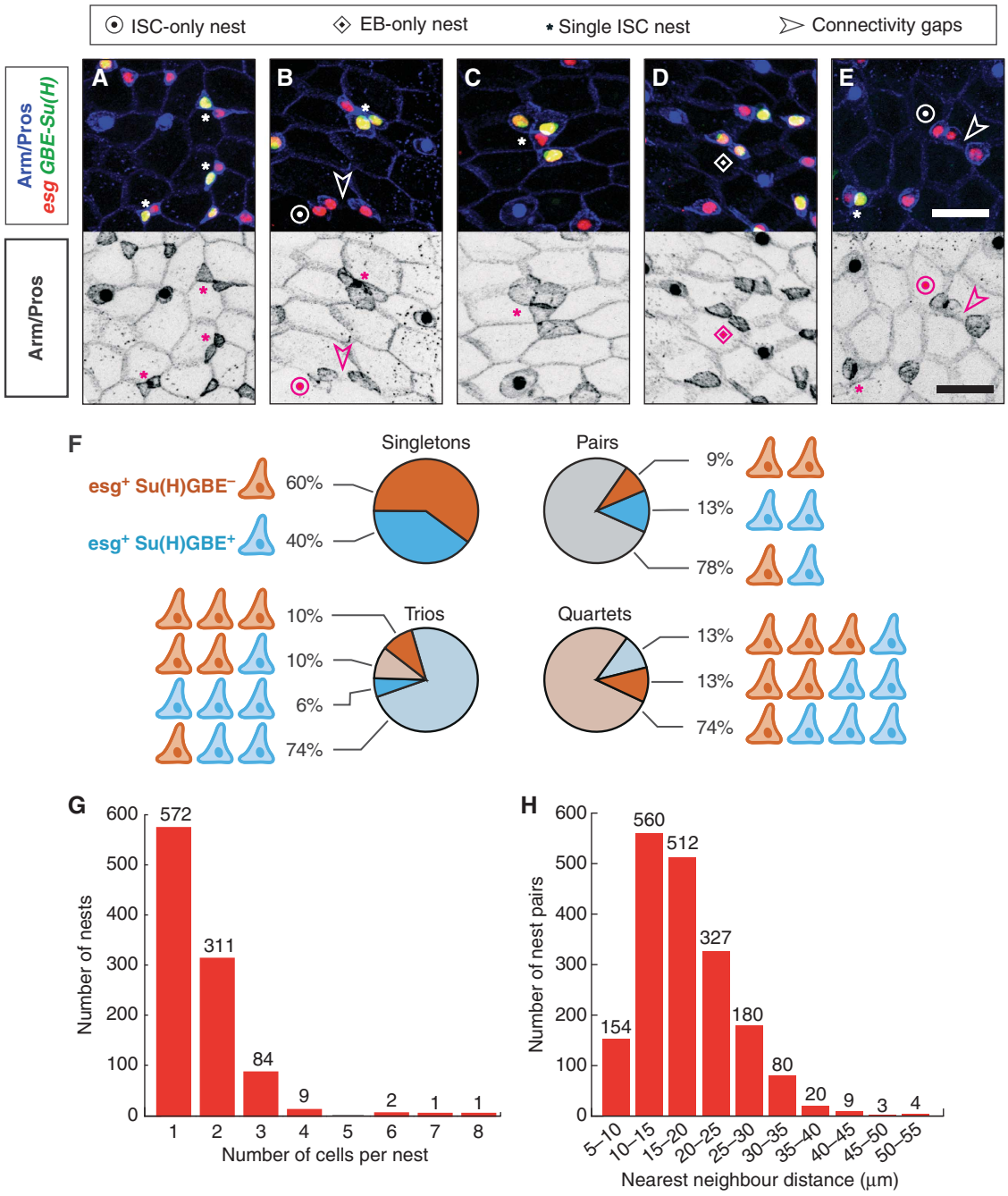

Figure 7 Nests of esg$^+$ cells are variable in composition and size. (**A–E**) esg$^+$ cell nests defined by Arm/β-catenin contacts (depicted separately in black/white panels). Bar in (**E**) is 20 μm. ISCs appear in red (esg$^+$) and EBs in yellow (esg$^+$ Su(H)GBE$^+$). (**A-C**) Nests containing one ISC and one (**A**), two (**B**) or three (**C**) EBs. (**D**, **E**) A two-EB and a two-ISC nest, respectively (see also **B**). Note in (**E**) the nearby ISC/EB pair demonstrating that Su(H)GBE-GFP signal was detectable in this field of view. Connectivity gaps between esg$^+$ cells are shown where relevant. (**F**) Relative frequencies of observed compositions, in ISCs and EBs, of the nests containing one to four cells. (**G**) Histogram depicting the observed counts of nest sizes. (**H**) Distances between nearest pairs of nests, binned in intervals of 5 μm.

relationships. We would expect to find ISCs predominantly closest to their siblings, even if their relative position could drift after division. When we considered the cell types of nearest pairs of esg$^+$ cells, we found that a majority were an ISC/EB pair (62% of 963 nearest pairs), with many nearest pairs of the same class (183 two-EBs and 179 two-ISCs), each corresponding to 19% of the total. This conforms with the observation that ~20% of Dl$^+$ cells are clustered in pairs (Jiang *et al*, 2009). Together, these results indicate that the spatial arrangement of ISCs and EBs is in general agreement with our observations of neutral drift and ISCs dividing in balanced proportions into two-ISCs, two-EBs or one ISC and one EB.

Dl/N signalling mediates neutral competition in the midgut

These results raise the question of the molecular basis for neutral competition in the midgut. This requires a unified

mechanism resulting in the three possible fate outcomes in a balanced manner. Since our model argues for extrinsic regulation, this mechanism should also be non-cell autonomous. Dl/N signalling is an obvious candidate, given its role in promoting EB differentiation (Micchelli and Perrimon, 2006; Ohlstein and Spradling, 2006, 2007; Maeda *et al*, 2008; Bardin *et al*, 2010; Liu *et al*, 2010; Perdigoto *et al*, 2011). Indeed, strong mutant conditions for either *N* or *Dl* prevent EB differentiation, while the cell-autonomous activation of *N* results in forced differentiation (Micchelli and Perrimon, 2006; Ohlstein and Spradling, 2006, 2007).

To test the ability of Dl/N to influence, in a non-cell autonomous manner, the balance of ISC division and differentiation, we took advantage of the sensitivity of Dl/N signalling to the dosage of *N*, and turned to mild mutant conditions where, in a Dl-dependent manner, N activity is either increased or decreased. We examined midguts from heterozygotes for three different alleles of *N*: N^{55e11}, a molecular null, and $l(1)N^{B}$ and N^{MCD1}, two gain of function alleles that exhibit increased, but Dl-sensitive, N activity (Brennan *et al*, 1997, 1999; Supplementary Figure S5). We used the ISC/EB ratio, which is precisely balanced in wild-type, homeostatic conditions (Micchelli and Perrimon, 2006; O'Brien *et al*, 2011; Wang *et al*, 2011; Figure 7) and is sensitive to variations in fate balance (O'Brien *et al*, 2011), as a read-out of the balanced proportions of recent division into two-ISCs, two-EBs or one ISC and one EB. The experiment was performed at 10 DOA, when wild-type flies are indisputably in homeostasis. Wild-type flies presented a perfect ISC:EB balance (ISC/EB = 1.03; Figure 8A), indistinguishable from the results at 3–5 DOA in Figure 7 (ISC/EB = 1.04; $P = 0.87$). However, for the $+/N^{55e11}$ heterozygotes, the ISC/EB ratio was imbalanced towards ISC (ISC/EB = 1.27). Conversely, in the two gain of function conditions $+/l(1)N^{B}$ and $+/N^{MCD1}$, the ratio was imbalanced towards EBs (ISC:EB ratios of 0.70 and 0.81, respectively; Figure 8A). The departure from ISC/EB balance in all mutant conditions is significant, with *P*-values of $\leqslant 0.003$ (Figure 8A). These results provide evidence that mild modulation of *N* signal can result in excessive ISC symmetric duplication or symmetric differentiation. In particular, the effect observed in these Dl dependent, gain of function conditions suggests that the ISC siblings can signal to each other.

Discussion

In this study, we have analysed long- and short-term lineage progression by size, survival and composition, and shown that *Drosophila* midgut is maintained by population asymmetry. This contrasts with a general notion in the field that homeostasis is based on the fate asymmetry of the ISC offpsring. Our results reveal that ISCs divide symmetrically in response to the differentiation and subsequent loss of a neighbouring ISC (or vice versa), which leads to neutral drift of the clonal population. We estimate that, in a context of fast turnover (two or three divisions per day), 2 in 10 divisions result in stem-cell loss and replacement. Our results further indicate that the fate of the ISC daughters might not be specified on division, but rather resolved through competition between proximate cells following division.

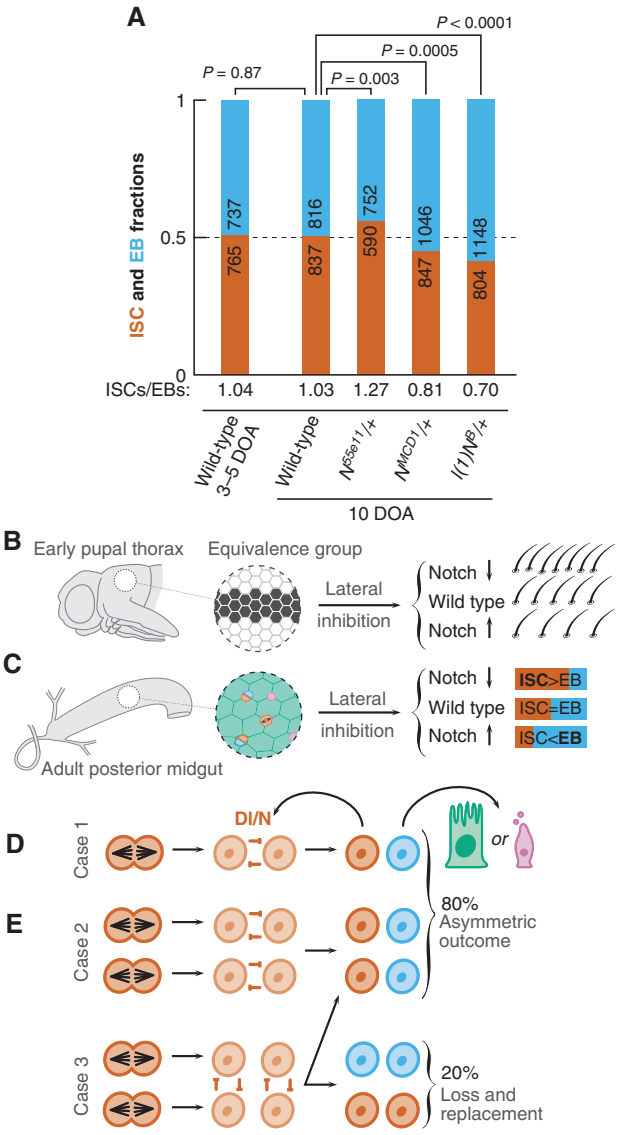

Figure 8 Population asymmetry in the midgut through lateral inhibition. (**A**) ISC/EB ratios in the different genetic backgrounds. Wild type presents a balanced proportion both at 3–5 DOA and at 10 DOA. Hypomorphic conditions for *N* ($N^{55e11}/+$) show excess ISCs, while hyperactive conditions ($l(1)N^{B}/+$ and $N^{MCD1}/+$) show increased number of EBs. (**B**) Lateral inhibition during the development of adult PNS restricts the number of sensory bristles arising in the dorsal thorax from a group of equivalence (black cells). Hypomorphic alleles of *N* lead to *neurogenic* phenotype (excess sensory bristles) whereas hyperactive *N* allelic combinations lead to *antineurogenic* phenotype (less bristles, in favour of epidermal fate). (**C**) Parallel phenomenology during the fate allocation of ISC offspring: 'neurogenic conditions' for *N* lead to excess of ISCs, whereas 'antineurogenic conditions' for *N* lead to less ISCs, in favour of EB fate. (**D**) During tissue maintenance, loss of mature cells is compensated by the differentiation of an EB cell combined with the division of an ISC. When an isolated ISC divides, competition can only occur between the siblings (case 1), leading to asymmetrical fate outcome. (**E**) If division occurs in two neighbouring ISCs, then there are two possible fate outcomes. If the competition to remain a stem cell occurs between sibling cells (case 2), then only one cell in each pair of daughter cells may differentiate leading to asymmetric fate outcome. However, if competition occurs between proximate non-sibling cells (case 3), then the fate outcome can result in either asymmetrical or symmetrical fate, the latter leading to ISC loss and replacement. From the results of the clonal analysis, we would predict that 2 out of 10 ISC divisions result in ISC loss and replacement.

Lateral inhibition as the molecular mechanism of neutral competition

The observation of neutral competition calls for the elucidation of its underlying molecular mechanism. By the nature of the process of neutral competition in this system, the associated mechanism must play a fundamental role in ISC self-renewal and EB commitment and be able to implement, non-cell autonomously, the stochastic resolution of binary fate decisions. Dl-N signalling fulfils both requirements: numerous experiments underpin its central role in the choice of commitment versus self-renewal in the midgut (Micchelli and Perrimon, 2006; Ohlstein and Spradling, 2006, 2007; Maeda *et al*, 2008; Bardin *et al*, 2010; Liu *et al*, 2010; Perdigoto *et al*, 2011), and studies of its function in neurogenesis have established an intrinsic ability to resolve stochastically binary choices of cell fate through the process of 'lateral inhibition', which involves reciprocal signalling between equivalent cells (reviewed in Simpson, 1990 and Greenwald, 1998).

The model of population asymmetry involves neutral competition between proximate cells (therefore based on extrinsic signals), which implies that ISC daughters are intrinsically equivalent at birth, and that fate is resolved after ISC division. Therefore, the ISC daughters are functionally equivalent and a good substrate for lateral inhibition, This is compatible with the observations that ISC daughter cells express N and they segregate Dl symmetrically (Ohlstein and Spradling, 2006, 2007). Furthermore, we provide evidence that this situation leads to mutual signalling. The excess of ISCs found in null and hypomorphic conditions for *N* (Micchelli and Perrimon, 2006; Ohlstein and Spradling, 2006; Perdigoto *et al*, 2011; Figure 8A) could be interpreted, in the framework of a unidirectional Dl signal from the ISC towards the EB, as a failure to implement the EB fate and a lapse into the 'default' ISC fate. However, this interpretation cannot account for the increased number of cells committing to EB fate in $+/l(1)N^{B}$ and $+/N^{MCD1}$ midguts (Figure 8A). These alleles exhibit Dl-dependent increased N signalling (Brennan *et al*, 1997; Supplementary Figure S5) which, in a scenario of unidirectional signalling, should not affect the balance of EB commitment. Rather, their phenotype suggests that both ISC daughters can receive Dl signal and reach the threshold of N activity for commitment. This is further highlighted by the parallel between the effects of these alleles on the ISC/EB ratio and on the development of peripheral nervous system (PNS) of *Drosophila*, a classical model for lateral inhibition (Simpson, 1990; Greenwald, 1998). In the PNS, a reduction of N activity, as in $+/N^{55e11}$, leads to *neurogenic* phenotypes with supernumerary sensory bristles, whereas excess of N activity, as in $+l(1)N^{B}$ and $+/N^{MCD1}$, results in *antineurogenic* phenotypes, with reduced number of bristles and more cells adopting the epidermal fate (Brennan *et al*, 1997; Ramain *et al*, 2001; Figure 8B and C). It is noteworthy that the molecular machinery that participates in Dl/N-mediated lateral inhibition in other contexts is also involved in ISC/EB fate decision (Bardin *et al*, 2010). With these elements, we propose that ISCs divide symmetrically, and the fate of the progeny is resolved through lateral inhibition mediated by Dl/N signalling (Figure 8D and E).

Lateral inhibition thus provides a straightforward way of implementing neutral competition. In many cases, Dl/N interaction will be restricted to sibling cells, the progeny of a single ISC division, and these cases will resolve into an ISC/EB asymmetric pair (Figure 8D). However, if in the course of tissue turnover the division of two ISCs occurred in close proximity, non-sibling cells could interact via Dl/N and engage in competition for the ISC fate through lateral inhibition. This in turn may lead to sibling cells adopting identical fates and therefore in ISC loss and replacement (Figure 8E). Such behaviour would translate precisely to the coupled events of loss and replacement implicit in the model (Supplementary Figure S4C), with the value of $2r$ weighting, combined, the chance of this contact and of its resolution into ISC loss and replacement. In this regard, the rich variety of esg^{+} cell nest composition in EB and ISC cells (Figure 7A–F), as well as the frequent proximity of ISC pairs (19% of nearest pairs), suggests that such encounters are possible in space. This may require nests to drift in position, but it is significant that, unlike other *Drosophila* adult stem cells, ISCs are not associated with niches having hub-like anatomical properties (reviewed in Losick *et al*, 2011).

Although our observations can, in principle, be explained solely as a result of lateral inhibition, we cannot rule out other mechanisms. In particular, the tissue could allow for a combination of either symmetric or intrinsically asymmetric divisions such that part of the ISC divisions that result in asymmetric fate could derive from either neutral competition or an intrinsic regulatory process. However, to conform with our observation that ISCs are equipotent, the stem-cell progeny of an intrinsically determined asymmetric cell division will have the same chance for loss and replacement in subsequent divisions as any other ISC. In other words, when facing their next division, all ISCs irrespective of their lineage history, would have to decide, stochastically, whether to undergo intrinsically asymmetric division, and, if they do not, the fate outcome of the division would be resolved again, stochastically, by extrinsically driven neutral competition. We find it difficult to conceive of a scenario for the molecular regulation of such a system.

Time window of homeostatic clonal expansion

Although the model provides an excellent fit to the early time course, the departure of the model at day 16 is significant. Although the clone size distribution conforms closely with the predicted scaling form (Figure 2C and E), consistent with the same underlying pattern of ISC fate, the overall average size of the surviving clones is smaller than predicted by a simple extrapolation of the fits to the earlier time point data with the same ISC loss/replacement rate (Figure 2E). The departure of theory and experiment may reflect a breakdown of homeostasis due to ageing. In particular, at this point of the clone chase the flies are 21–23 days old (see Supplementary Methods and Supplementary Figure S6A), an age at which ageing-related non-homeostatic phenotypes can be detected in the midgut (Biteau *et al*, 2008). Indeed, such behaviour might be explained by a shift towards uncompensated loss of terminally differentiated cells, consistent with the fact that the clone density continues to fall, and in a manner consistent with theory (Figure 2A). Alternatively, it is also possible that the heat shock, which does not produce damage leading to detectable alteration of the tissue size or cell density (Supplementary Figure S6B and C), instead triggers the acceleration of tissue turnover, an effect that would last at

least 8 days, but less than 16. This effect could be similar, but milder, to that observed in the recently described *Drosophila* gastric adult stem cells, which show a sharp activation of homeostatic turnover in response to heat shock (Strand and Micchelli, 2011). This view is supported by the observation that the mitotic index in the posterior midgut is, after heat-based clonal induction, higher than in untreated organs (Lin *et al*, 2008; Beebe *et al*, 2010; Shaw *et al*, 2010).

Parallels with mammalian intestinal homeostasis

There are similarities between the *Drosophila* midgut and mammalian intestine at the levels of cell biology and genetics (Casali and Batlle, 2009). Our study adds a new parallel from the perspective of their strategy for homeostatic maintenance. In humans, studies of methylation patterns point at stem-cell loss and replacement in the intestinal crypt (reviewed in Kim and Shibata, 2002) and in the mouse, using an approach similar to that employed here, recent studies have shown that the intestinal crypt is maintained by an equipotent $Lgr5^+$ stem-cell population in which the loss of cells from the stem-cell compartment is compensated by the symmetric multiplication of neighbours (López-García *et al*, 2010; Snippert *et al*, 2010). Further evidence suggests that stem-cell competence in the small intestine is ensured by proximity to Paneth cells, which aggregate throughout the crypt base (Sato *et al*, 2011). As tissue is turned over, $Lgr5^+$ cells undergo neutral competition resulting in a progression towards crypt monoclonality. At longer timescales, crypts undergo fission, leading to a further 'coarsening' of the clonal population. We speculate that in *Drosophila*, the esg^+ nests fulfil a function analogous to intestinal crypts, playing host to a much smaller equipotent cell population, and undergoing fission with a far greater frequency. However, in contrast with intestinal crypt, it appears that ISC competence in *Drosophila* does not require a separate niche-supporting cell.

In summary, our studies show that, in *Drosophila*, adult midgut homeostasis follows a pattern of population asymmetry involving an equipotent population of ISCs. ISC division may result in any of all three possible fate outcomes leading to asymmetric fate (ISC/EB), symmetric duplication (two ISCs), or symmetric differentiation (two EBs), the latter two balanced in frequency. These findings point at a mechanism involving lateral inhibition and provide a natural framework to explain regeneration following injury or infection.

Materials and methods

Drosophila culture

Flies were raised and maintained on standard cornmeal/yeast medium at 25°C unless specifically indicated. Experiments were conducted in well-fed, mated females. See Supplementary Methods for genotypes.

Analysis of esg^+ cell nests and ISC/EB balance

esg-lacZ; Su(H)GBE-GFP:nls flies at 3–5 DOA (N^+) and 10 DOA ($N^*/+$) were dissected and probed for LacZ (10DOA), or LacZ, Arm/β-catenin and Pros (3–5 DOA). With ImageJ, confocal z-stacks were z-projected and we manually recorded the position the esg^+ nuclei (PointPicker), identified groups of esg^+ cells sharing at least a common apical vertex, and binarized the Su(H)GBE-GFP signal (Entropy Threshold). Nest position was determined as the average position of the component nuclei.

Long-term lineage chase

tub-FRT-lacZ flies aged 5–7 days were induced by 30-min treatment at 37°C. At each time point (1, 2, 3, 4, 5, 8, 16 and 28 days after induction), ~40 flies were dissected and stained for LacZ, F-actin and DNA. The F-actin signal was used to estimate the amount of screened tissue, using usual anatomical landmarks to define the boundaries of the posterior midgut (Supplementary Methods). Clones were imaged as z-stacks spanning all the labelled cells, and the size recorded manually. For each time point, we collected ~100 clones from at least 10 different organs, except for day 16 (Supplementary Table S3). We made a number of observations to validate the accuracy of the method (Supplementary Methods). In particular, we verified that the tissue was in homeostasis (Supplementary Figure S6), the specificity of the induction (Supplementary Figure S2A), the temporal and spatial response of the tissue to induction (Supplementary Figure S2C and D; Figure 3A and B) and the precision of clone identification (Supplementary Figure S2B).

Short-term lineage chases

tub-FRT-lacZ flies aged 3–6 days were induced for 40 min at 38°C, dissected 2–5 days after induction and stained for LacZ, Dl and Pros. We recorded the total number of cells and those positive for Dl and Pros, and those that were putative polyploid and diploid, according to an empirical threshold diameter (7 μm).

For the 28-h lineage chase, flies aged 5–7 days were induced for 60 min at 37°C, stained for Dl and recorded accordingly. The clonal fates were disclosed in their history of symmetric and asymmetric divisions, maximizing the asymmetric history in the cases where fate was ambiguous (Figure 6A and C).

Twin-spot analyses

Flies were raised and aged at 18°C to avoid spurious induction, and induced for 20 min at 34°C (twin-spot generator) and 60 min at 37°C (the other two). Clones were grown at 25°C for 2–3 days before dissection. Twin-spot MARCM seemed the most suitable in promoter homogeneity and induction specificity (Supplementary Methods).

Antibody staining and microscopy

Stainings were performed as in Bardin *et al* (2010). Primary antibodies were rabbit anti-βGal (Cappel, 1:10 000), chicken anti-GFP (Abcam, 1:2000), rabbit anti-RFP (Clontech, 1:250), mouse anti-Dl (C594-9B ascites, DSHB, 1:2000), rabbit anti-Pros (Vaessin *et al*, 1991; 1:2000) and mouse anti-Pros (mAb MR1A, DSHB, 1:50). Secondary antibodies were from Invitrogen or Jackson. DNA dyes were DAPI or TO-PRO-3 (Invitrogen). F-actin staining was phalloidin-FITC (Sigma, 1:50) or phalloidin-Alexa568 (Invitrogen, 1:500). Mounting media were Vectashield or 4% *N*-propyl-galate, 80% glycerol. Images were acquired with Zeiss LSM and Leica SP confocal systems. Images and figures were assembled using ImageJ, Adobe Photoshop and Illustrator.

Supplementary data

Supplementary data are available at *The EMBO Journal* Online (http://www.embojournal.org).

Acknowledgements

We are grateful to François Schweisguth and Marcos González-Gaitán for valuable discussions and constructive criticisms, Pablo J Barrecheguren-Manero for technical assistance, members of the AMA laboratory for critical reading and anonymous reviewers for suggestions to improve the manuscript. Work by AMA, JdN and YB is supported by the Wellcome Trust. JdN and BDS acknowledge EPSRC grant no. EP/032773/1.

Author contributions: AMA and BDS conceived the project. JdN, CNP and YB performed the experiments and collected the data. MHS produced the *Su(H)GBE-GFP:nls* flies. BDS performed the quantitative analysis. JdN and BDS analysed the results and wrote the paper. AMA and AJB discussed the results and commented on the manuscript.

Conflict of interest

The authors declare that they have no conflict of interest.

References

Apidianakis Y, Rahme LG (2011) Drosophila melanogaster as a model for human intestinal infection and pathology. *Dis Model Mech* **4:** 21–30

Bardin AJ, Perdigoto CN, Southall TD, Brand AH, Schweisguth F (2010) Transcriptional control of stem cell maintenance in the Drosophila intestine. *Development* **137:** 705–714

Beebe K, Lee WC, Micchelli CA (2010) JAK/STAT signaling coordinates stem cell proliferation and multilineage differentiation in the Drosophila intestinal stem cell lineage. *Dev Biol* **338:** 28–37

Biteau B, Hochmuth CE, Jasper H (2008) JNK activity in somatic stem cells causes loss of tissue homeostasis in the aging Drosophila gut. *Cell Stem Cell* **3:** 442–455

Biteau B, Jasper H (2011) EGF signaling regulates the proliferation of intestinal stem cells in Drosophila. *Development* **138:** 1045–1055

Brennan K, Tateson R, Lewis K, Arias AM (1997) A functional analysis of Notch mutations in Drosophila. *Genetics* **147:** 177–188

Brennan K, Tateson R, Lieber T, Couso JP, Zecchini V, Arias AM (1999) The abruptex mutations of notch disrupt the establishment of proneural clusters in Drosophila. *Dev Biol* **216:** 230–242

Buchon N, Broderick NA, Kuraishi T, Lemaitre B (2010) Drosophila EGFR pathway coordinates stem cell proliferation and gut remodeling following infection. *BMC Biol* **8:** 152

Casali A, Batlle E (2009) Intestinal stem cells in mammals and Drosophila. *Cell Stem Cell* **4:** 124–127

Choi NH, Lucchetta E, Ohlstein B (2011) Nonautonomous regulation of Drosophila midgut stem cell proliferation by the insulin-signaling pathway. *Proc Natl Acad Sci USA* **108:** 18702–18707

Clayton E, Doupe DP, Klein AM, Winton DJ, Simons BD, Jones PH (2007) A single type of progenitor cell maintains normal epidermis. *Nature* **446:** 185–189

Cohen M, Georgiou M, Stevenson NL, Miodownik M, Baum B (2010) Dynamic filopodia transmit intermittent Delta-Notch signaling to drive pattern refinement during lateral inhibition. *Dev Cell* **19:** 78–89

De Joussineau C, Soule J, Martin M, Anguille C, Montcourrier P, Alexandre D (2003) Delta-promoted filopodia mediate long-range lateral inhibition in Drosophila. *Nature* **426:** 555–559

Fox DT, Spradling AC (2009) The Drosophila hindgut lacks constitutively active adult stem cells but proliferates in response to tissue damage. *Cell Stem Cell* **5:** 290–297

Fre S, Bardin A, Robine S, Louvard D (2011) Notch signaling in intestinal homeostasis across species: the cases of *Drosophila*, Zebrafish and the mouse. *Exp Cell Res* **317:** 2740–2747

Greenwald I (1998) LIN-12/Notch signaling: lessons from worms and flies. *Genes Dev* **12:** 1751–1762

Griffin R, Sustar A, Bonvin M, Binari R, del Valle Rodriguez A, Hohl AM, Bateman JR, Villalta C, Heffern E, Grunwald D, Bakal C, Desplan C, Schubiger G, Wu CT, Perrimon N (2009) The twin spot generator for differential Drosophila lineage analysis. *Nat Methods* **6:** 600–602

Harrison DA, Perrimon N (1993) Simple and efficient generation of marked clones in Drosophila. *Curr Biol* **3:** 424–433

Hou SX (2010) Intestinal stem cell asymmetric division in the Drosophila posterior midgut. *J Cell Physiol* **224:** 581–584

Jiang H, Edgar BA (2009) EGFR signaling regulates the proliferation of Drosophila adult midgut progenitors. *Development* **136:** 483–493

Jiang H, Edgar BA (2011) Intestinal stem cells in the adult Drosophila midgut. *Exp Cell Res* **317:** 2780–2788

Jiang H, Grenley MO, Bravo MJ, Blumhagen RZ, Edgar BA (2011) EGFR/Ras/MAPK signaling mediates adult midgut epithelial homeostasis and regeneration in Drosophila. *Cell Stem Cell* **8:** 84–95

Jiang H, Patel PH, Kohlmaier A, Grenley MO, McEwen DG, Edgar BA (2009) Cytokine/Jak/Stat signaling mediates regeneration and homeostasis in the Drosophila midgut. *Cell* **137:** 1343–1355

Karpowicz P, Perrimon N (2010) All for one, and one for all: the clonality of the intestinal stem cell niche. *F1000 Biol Rep* **2:** 73

Kim KM, Shibata D (2002) Methylation reveals a niche: stem cell succession in human colon crypts. *Oncogene* **21:** 5441–5449

Klein AM, Nakagawa T, Ichikawa R, Yoshida S, Simons BD (2010) Mouse germ line stem cells undergo rapid and stochastic turnover. *Cell Stem Cell* **7:** 214–224

Klein AM, Simons BD (2011) Universal patterns of stem cell fate in cycling adult tissues. *Development* **138:** 3103–3111

Lee WC, Beebe K, Sudmeier L, Micchelli CA (2009) Adenomatous polyposis coli regulates *Drosophila* intestinal stem cell proliferation. *Development* **136:** 2255–2264

Lin G, Xu N, Xi R (2008) Paracrine Wingless signalling controls self-renewal of Drosophila intestinal stem cells. *Nature* **455:** 1119–1123

Lin G, Xu N, Xi R (2009) Paracrine unpaired signaling through the JAK/STAT pathway controls self-renewal and lineage differentiation of drosophila intestinal stem cells. *J Mol Cell Biol* **2:** 37–49

Lin G, Xu N, Xi R (2010) Paracrine unpaired signaling through the JAK/STAT pathway controls self-renewal and lineage differentiation of drosophila intestinal stem cells. *J Mol Cell Biol* **2:** 37–49

Liu W, Singh SR, Hou SX (2010) JAK-STAT is restrained by Notch to control cell proliferation of the Drosophila intestinal stem cells. *J Cell Biochem* **109:** 992–999

López-García C, Klein AM, Simons BD, Winton DJ (2010) Intestinal stem cell replacement follows a pattern of neutral drift. *Science* **330:** 822–825

Losick VP, Morris LX, Fox DT, Spradling A (2011) Drosophila stem cell niches: a decade of discovery suggests a unified view of stem cell regulation. *Dev Cell* **21:** 159–171

Maeda K, Takemura M, Umemori M, Adachi-Yamada T (2008) E-cadherin prolongs the moment for interaction between intestinal stem cell and its progenitor cell to ensure Notch signaling in adult Drosophila midgut. *Genes Cells* **13:** 1219–1227

Micchelli CA, Perrimon N (2006) Evidence that stem cells reside in the adult Drosophila midgut epithelium. *Nature* **439:** 475–479

Miller A (1950) The internal anatomy and histology of the imago of Drosophila melanogaster. In: *Biology of Drosophila*, Demerec M (ed.) pp. 420–534, Hafner, New York

O'Brien LE, Soliman SS, Li X, Bilder D (2011) Altered modes of stem cell division drive adaptive intestinal growth. *Cell* **147:** 603–614

Ohlstein B, Spradling A (2006) The adult Drosophila posterior midgut is maintained by pluripotent stem cells. *Nature* **439:** 470–474

Ohlstein B, Spradling A (2007) Multipotent Drosophila intestinal stem cells specify daughter cell fates by differential notch signaling. *Science* **315:** 988–992

Perdigoto CN, Schweisguth F, Bardin AJ (2011) Distinct levels of Notch activity for commitment and terminal differentiation of stem cells in the adult fly intestine. *Development* **138:** 4585–4595

Potten CS (1974) The epidermal proliferative unit: the possible role of the central basal cell. *Cell Tissue Kinet* **7:** 77–88

Potten CS (1981) Cell replacement in epidermis (keratopoiesis) via discrete units of proliferation. *Int Rev Cytol* **69:** 271–318

Ramain P, Khechumian K, Seugnet L, Arbogast N, Ackermann C, Heitzler P (2001) Novel Notch alleles reveal a Deltex-dependent pathway repressing neural fate. *Curr Biol* **11:** 1729–1738

Sato T, van Es JH, Snippert HJ, Stange DE, Vries RG, van den Born M, Barker N, Shroyer NF, van de Wetering M, Clevers H (2011) Paneth cells constitute the niche for Lgr5 stem cells in intestinal crypts. *Nature* **469:** 415–418

Shaw RL, Kohlmaier A, Polesello C, Veelken C, Edgar BA, Tapon N (2010) The Hippo pathway regulates intestinal stem cell proliferation during Drosophila adult midgut regeneration. *Development* **137:** 4147–4158

Simpson P (1990) Lateral inhibition and the development of the sensory bristles of the adult peripheral nervous system of Drosophila. *Development* **109:** 509–519

Snippert HJ, van der Flier LG, Sato T, van Es JH, van den Born M, Kroon-Veenboer C, Barker N, Klein AM, van Rheenen J, Simons BD, Clevers H (2010) Intestinal crypt homeostasis results from neutral competition between symmetrically dividing Lgr5 stem cells. *Cell* **143:** 134–144

Spradling AC, Stern D, Beaton A, Rhem EJ, Laverty T, Mozden N, Misra S, Rubin GM (1999) The Berkeley Drosophila genome project gene disruption project: Single P-element insertions mutating 25% of vital Drosophila genes. *Genetics* **153:** 135–177

Strand M, Micchelli CA (2011) Quiescent gastric stem cells maintain the adult Drosophila stomach. *Proc Natl Acad Sci USA* **108:** 17696–17701

Vaessin H, Grell E, Wolff E, Bier E, Jan LY, Jan YN (1991) Prospero is expressed in neuronal precursors and encodes a nuclear protein that is involved in the control of axonal outgrowth in Drosophila. *Cell* **67:** 941–953

Wang L, McLeod CJ, Jones DL (2011) Regulation of adult stem cell behavior by nutrient signaling. *Cell Cycle* **10:** 2628–2634

Watt FM, Hogan BL (2000) Out of Eden: stem cells and their niches. *Science* **287:** 1427–1430

Xu N, Wang SQ, Tan D, Gao Y, Lin G, Xi R (2011) EGFR, Wingless and JAK/STAT signaling cooperatively maintain Drosophila intestinal stem cells. *Dev Biol* **354:** 31–43

Yu HH, Chen CH, Shi L, Huang Y, Lee T (2009) Twin-spot MARCM to reveal the developmental origin and identity of neurons. *Nat Neurosci* **12:** 947–953